International Journal of Mass Spectrometry 287 (2009) 32–38

Contents lists available at ScienceDirect

International Journal of Mass Spectrometry

journal homepage: www.elsevier.com/locate/ijms

FT-ICR MS optimization for the analysis of intact proteins

Aleksey V. Tolmachev, Errol W. Robinson, Si Wu, Ljiljana Paša-Tolić*, Richard D. Smith

Biological Sciences Division, Pacific Northwest National Laboratory P.O. Box 999, Richland, WA, 99352, United States

ARTICLE INFO

Article history:
Received 3 July 2008
Received in revised form 15 October 2008
Accepted 17 October 2008
Available online 1 November 2008

Keywords:
FT-ICR
Top-down proteomics
Dynamic range
Resolution
Mass accuracy

ABSTRACT

Fourier-transform ion cyclotron resonance (FT-ICR) mass spectrometry (MS) remains the technique of choice for the analysis of intact proteins from complex biological systems, i.e., top-down proteomics. Recently, we have implemented a compensated open cylindrical ion trapping cell into a 12 T FT-ICR mass spectrometer. This new cell has previously demonstrated improved sensitivity, dynamic range, and mass measurement accuracy for the analysis of relatively small tryptic peptides. These improvements are due to the modified trapping potential of the cell which closely approximates the ideal harmonic trapping potential. Here, we report the instrument optimization for the analysis of large macro-molecular ions, such as proteins. Single transient mass spectra of multiply charged bovine ubiquitin ions with sub-ppm mass measurement accuracy, improved signal intensity, and increased dynamic range were obtained using this new cell with increased post-excitation cyclotron radii. The increased cyclotron radii correspond to increased ion kinetic energy and collisions between neutrals and ions with sufficient kinetic energy can exceed a threshold of single collision ion fragmentation. A transition then occurs from relatively long signal lifetimes at low excitation radii to potentially shorter lifetimes, defined by the average ion-neutral collision time. The proposed high energy ion loss mechanism is evaluated and compared with experimental results for bovine ubiquitin and serum albumin. We find that the analysis of large macro-molecules can be significantly improved by the further reduction of pressure in the ion trapping cell. This reduces the high energy ion losses and can enable increased sensitivity and mass measurement accuracy to be realized without compromising resolution. Further, these results appear to be generally applicable to FTMS, and it is expected that the high energy ion loss mechanism also applies to Orbitrap mass analyzers.

1. Introduction

Fourier-transform ion cyclotron (FT-ICR) mass spectrometry (MS) continues to deliver the highest mass resolving power and mass measurement accuracy (MMA). FT-ICR MS is uniquely suited for the analysis of complex natural mixtures, such as, fossil [1,2] and bio-fuels [3], biological imaging [4], metabolomics [5], and proteomics [6,7]. The characterization of biological systems through the analysis of intact proteins [8,9] and protein complexes [10] with FT-ICR MS, e.g., top-down proteomics, continues to reveal the complex and dynamic nature of biological systems [11,12]. Characterization of post-translational modifications (PTM) plays an important role in understanding the regulation and control of biological systems. Top-down proteomic analysis effectively characterizes the number of PTMs, how PTMs change between biological system states, and correlations between PTMs. Characterization of proteomes through the analysis of intact proteins continues to progress with improvements in instrumentation and methodology such as the demonstrated analysis of over 100 kDa proteins [13] and LC-MS of complex proteomes [9,11,12].

We are customizing a 12 Tesla FT-ICR mass spectrometer for top-down proteomics applications, which require intact protein MS measurements of molecular masses greater than 100 kDa, with isotopic resolution, ppm range MMA and optimally high sensitivity and dynamic range. The instrument has been upgraded with a new trapped ion cell possessing a close to ideal DC trapping potential, enabling increased ion excitation powers, and thus reduced space charge effects along with improved MMA, sensitivity and dynamic range [14]. Initial experimental characterization of the new cell confirmed the improved performance for conditions typical to bottom-up proteomics measurements, for a range of molecular masses characteristic for tryptic peptides, up to ~3 kDa [14]. Here we report the characterization of the new cell for the analysis of intact proteins based on a consideration of the fundamental factors involved in the high resolution measurements of macro-molecular ions and a comparison with experimental results that support these insights. Analysis of the theoretical and experimental results suggests additional possibilities for further optimization of the FT-ICR

* Corresponding author. Tel.: +1 509 376 8859; fax: +1 509 376 2303.
E-mail address: ljiljana.pasatolic@pnl.gov (L. Paša-Tolić).

1387-3806/$ – see front matter © 2008 Elsevier B.V. All rights reserved.
doi:10.1016/j.ijms.2008.10.010

MS instrumentation for the analysis of large molecules such as, intact proteins.

2. Experimental

2.1. Cell design

Briefly, the compensated [15] cylindrical cell [16,17] used for the experiments reported here has additional trapping electrode segments to generate an electric field for ion confinement which is significantly closer to the ideal harmonic trapping potential [18]. Extensive theoretical considerations were made in generating the compensated cylindrical cell design as previously reported [14]. Previous experiments comparing the compensated cell with a standard open cell configuration demonstrated significant improvements for the compensated cell in sensitivity, MMA, and dynamic range for the analysis of tryptic peptides [14]. These improvements were based on the design of the compensated cell maximizing the benefits of greater excitation radius while minimizing deleterious effects.

2.2. Data acquisition

Bovine ubiquitin and serum albumin were acquired from Sigma–Aldrich (St. Louis, MO) and used as received. Mass spectra for direct infusion experiments were acquired on a modified [11] Bruker 12 Tesla FT-ICR mass spectrometer (Bruker Daltonics, Billerica, MA) using electrospray ionization of a 1.0 μM ubiquitin from a solution of 1:1 water: methanol with 2% acetic acid.

Mass spectra of this solution were acquired over a range of excitation powers, external accumulation times, and cell trapping voltages in automated fashion using Xmass (Bruker Daltonics, Billerica, MA) scripts. Typical values for results reported here were 0.06 s for external accumulation and 2.0 V for cell trapping voltage. Mass spectra were acquired with excitation attenuation ranging from 0 to 16 dB. Peak to peak excitation voltages of 260, 150, 93, 61, 37 V corresponded to excitation attenuations of 0, 4, 8, 12, 16 dB. Results with differing accumulation times and trapping potentials follow the same reported trends. Mass spectra were obtained at an approximate pressure of 1×10^{-10} and 3×10^{-10} Torr. Mass spectra at 3×10^{-10} Torr were obtained after one initial bake-out and pump down after insertion of the new cell. Subsequent baking and pump down time resulted in a lower base pressure of 1×10^{-10} Torr. The measured UHV pressure is expected to be somewhat lower than the actual pressure in the ion trapping cell due to the positioning of the ion gauge relatively closer to the UHV turbo molecular pump than the ICR trapping cell. However, the relative difference between measured pressure values should correspond to the relative difference of the pressure in the ion trapping cell. The ion gauge was calibrated while in the magnetic field during initial construction of the mass spectrometer. External accumulation was performed in the standard Bruker hexapole with a short pulse of gas to increase trapping efficiency. Collections of spectra were processed using in-house developed software to characterize instrument performance. Each transient was zero-filled twice, Fourier-transformed, and converted to the m/z domain.

Reverse phase LC-MS was performed at 10,000 psi on a 60 cm × 75 μm column packed in-house with C5 stationary phase Phenomenex Jupiter 5 μm particles (Phenomenex, Torrance, CA) [11,12]. Mobile phase A was 0.05% trifluoroacetic acid, 0.2% acetic acid, 25% acetonitrile, 5% isopropanol, and 69.75% water while mobile phase B was 0.05% trifluoacetic acid, 9.95% water, 45% acetonitrile, and 45% isopropanol. Mass spectra for LC-MS were acquired from a 1.0 μg injection of bovine serum albumin (BSA) in solvent A onto the reverse phase column.

3. Results and discussion

3.1. Characterization of the compensated cell

Optimization of the new compensated cylindrical cell for macromolecular ions used automated scripts that produced mass spectra in a range of excitation powers covering post-excitation radii up to the maximum possible radius R_{max} (i.e., approximately the inner cell radius, R_{max} = 3 cm). The procedure was used previously for an initial cell characterization using a mixture of peptides [14]. In this work we have used seven of the typically observed ubiquitin charge states. Fig. 1 shows a sample single mass spectrum of ubiquitin obtained with the compensated cell with an external accumulation time of 0.06 s and an excitation attenuation of 7 dB.

By regulating the DC trapping potential applied to each trapping segment of the new ion trapping cell, the optimum compensated electrode configuration can be compared to the standard open cylindrical cell configuration [14]. Fig. 2 shows the total ion current (TIC) profile of mass spectra obtained for a range of excitation powers for both the compensated and standard open cell configurations at an approximate pressure of 1×10^{-10} Torr. Increased TIC is observed for the compensated cell configuration at higher excitation radii relative to the standard open cell configuration. Note that an excitation attenuation of 3 dB corresponds to $\sim 0.75 R_{max}$ [14]. The TIC improvement obtained with the compensated cell is less pronounced for ubiquitin than for previously reported peptide mass spectra [14]. Observation of the positive effect of electric field compensation on the transient life time requires the UHV pressure to be sufficiently low. To illustrate this behavior, Fig. 2 also shows the TIC profile for the compensated cell at a relatively higher pressure of 3×10^{-10} Torr. (The TIC values for mass spectra at $\sim 3 \times 10^{-10}$ Torr were scaled to facilitate comparisons in TIC trends between the differing pressures). With the cell pressure increased by a factor of 3, the two cell configurations produced similar results (data for the standard open cell configuration at higher pressure not shown). This can be attributed to the transient life times defined by the ion-neutral collision rate, rather than by the harmonicity of the trapping potential, see discussion below.

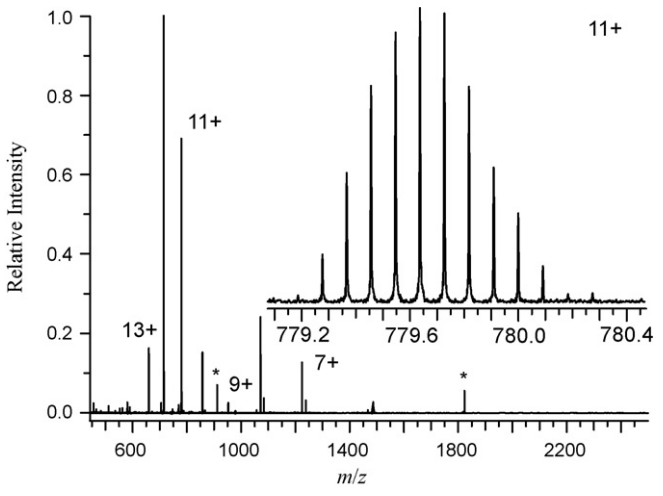

Fig. 1. ESI mass spectrum of ubiquitin obtained using the compensated cell, with an excitation attenuation of 7 dB, from a single transient 1.3 s long, with resolution of ~230,000 and insert detail of the 11+ charge state.

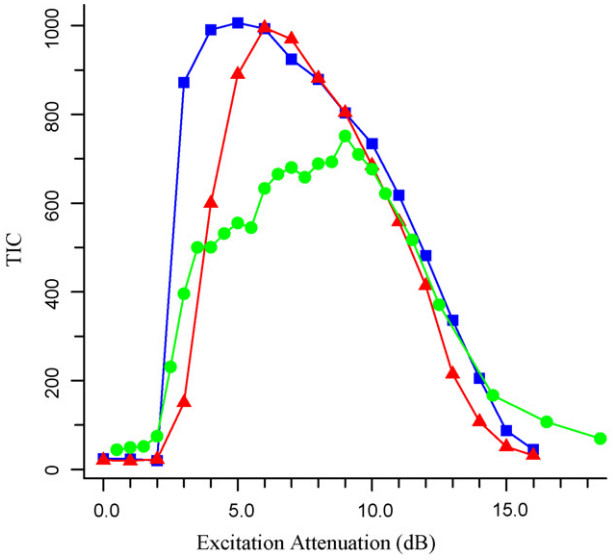

Fig. 2. Total ion current (TIC) versus excitation power (plotted in terms of attenuation, dB) for the compensated cell configuration, spectra were acquired at $\sim 1 \times 10^{-10}$ Torr (squares), open cell configuration, $\sim 1 \times 10^{-10}$ Torr (triangles), and compensated cell configuration at an increased pressure of $\sim 3 \times 10^{-10}$ Torr (circles).

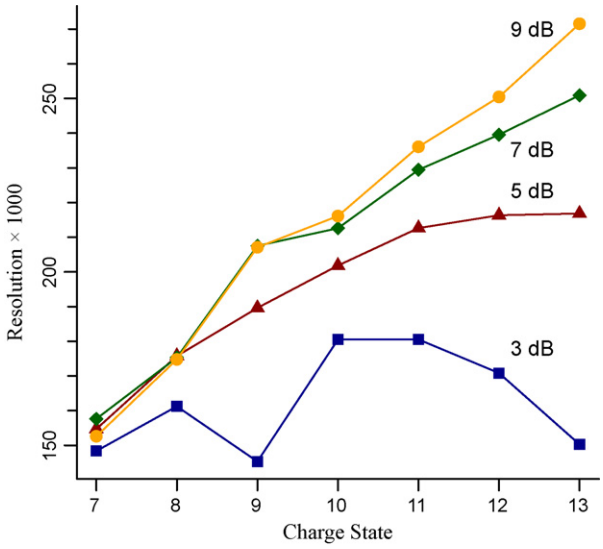

Fig. 4. Resolution of ubiquitin 7 to 13+ obtained at excitation attenuations of 9 dB (circles), 7 dB (diamonds), 5 dB (triangles), and 3 dB (squares) corresponding to approximately 0.4, 0.5, 0.6, and 0.75 of the maximum cell radius, R_{max}, of ~3.0 cm.

Because the observed increase in TIC with the more ideal trapping potential of the compensated cell is due to improved coherence of the excited ion cloud, the mass measurement accuracy (MMA) of the compensated cell also improves relatively to the standard open cell configuration [14]. The MMA improvement observed for the compensated cell with increasing excitation power, Fig. 3, can be attributed to decreased space charge effects at larger excitation radii, consistent with earlier results obtained for the peptide calibration mixture [14]. Improved MMA can also be attributed to higher S/N at higher excitation radius, however we do not expect this to be significant, since the trends were reproducibly obtained for a wide range of ion populations and S/N ratios [14]. Note that without the compensation of the trapping potential to a more ideal harmonic trapping field, the MMA does not improve at increased excitation radii as demonstrated by the standard open cell configuration results, Fig. 3. This is due to radial electric fields of the standard open cell configuration having deleterious effects to the ion cloud coherence and motion. Such effects typically become more pronounced at increased excitation radii. Also, the demonstrated improvements of MMA for the compensated cell are not due to external calibration artifacts as the MMA of each mass spectrum was estimated using ubiquitin charge states as internal calibrants. Thus, when the compensated cell is used, increased excite power conditions (3 dB) resulted in optimizing MMA while also maximizing sensitivity, as indicated by TIC. The mass accuracy trends obtained for ubiquitin, Fig. 3, are similar to peptide mixture mass accuracy results that used more detailed dB increments (0.5) and a range of different ion populations [14].

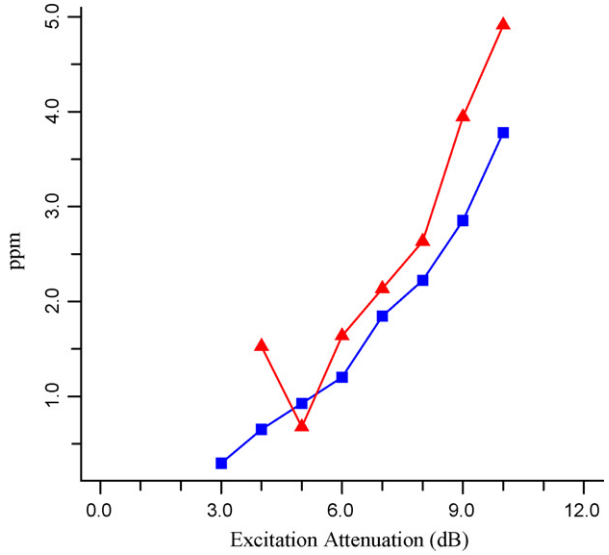

Fig. 3. Mass measurement error, plotted as ppm, versus excitation power, plotted in terms of attenuation dB, for the compensated cell configuration (squares) and open cell configuration (triangles). The internal calibration using 6 charge states of ubiquitine was used for the mass measurement error calculation.

Another critical attribute of intact protein MS measurements is mass resolving power, which should be sufficient to resolve isotopic structure. Fig. 4 shows resolving power as a function of charge state obtained at 4 different excite powers which result in excitation radii ranging from ~0.4 to ~0.75R_{max}. The observed decrease in resolution with increased excitation power (i.e., lower dB) can be attributed, in part, to an increased contribution of magnetron frequency dispersion due to deviations from the quadrupolar trapping potential. Another factor is the shorter life time of the ion signal due to an increased rate of the ion neutral collisions [19]. Note that, due to lower intensity, the resolution estimated for 9+ ions has additional uncertainty. The following calculations estimate the contribution of ion neutral collisions to the observed resolution.

3.2. Estimations of the ion signal lifetime

The velocity of ion motion during detection, v, can be estimated via the cyclotron frequency ω (angular units) and the post-excitation cyclotron radius r_c as follows:

$$v = \omega r_c \tag{1}$$

The unperturbed cyclotron frequency can be used for this approximate estimation:

$$\omega = \left(\frac{ze}{m}\right) B \tag{2}$$

where, the ion charge is expressed via the charge state z and the elementary charge e, m is the ion mass, and B is the magnetic field intensity. The characteristic time between ion neutral collisions, t_{coll}, can be estimated as the inverse collision frequency, using the cross section, Ω, of the ubiquitin ion:

$$t_{coll} = \frac{1}{(n v \Omega)} \tag{3}$$

The ubiquitin ion cross section is dependent on many factors such as, ion charge state, initial solution conditions, ion heating during desolvation and transport into the ion cell, etc. For present purposes, an approximate value of 1600 Å^2 will be used for Ω [20]. Using a B of 12 Tesla, r_c of 2 cm, the gas number density corresponding to the pressure 1×10^{-10} Torr, and an ion charge state, z of 10, we obtain the following quantities:

$$\omega = 2\pi \times 215\,\text{kHz}$$

$$v = 2.7 \times 10^4\,\text{m/s}$$

$$t_{coll} = 0.66\,\text{s} \tag{4}$$

The result of an ion neutral collision depends on the kinetic energy as follows. A low energy collision between a macromolecular ion, with m of 8560 Da, and a small neutral molecule, with m_g of 28 Da, results in a minor change in the magnitude and direction of the pre-collision ion velocity. Thus, multiple ion neutral collisions may be needed to de-phase the ion motion from the cohesive forces arising from the excited coherent ion cloud motion. Alternatively, above a certain threshold of ion kinetic energy, a single ion neutral collision may result in ion fragmentation, which would immediately exclude the ion from the coherent ion cloud. Such high energy collisions should result in the observed signal life times for the excited coherent ion cloud being defined by Eq. (3).

The kinetic energy of the post-excitation cyclotron ion motion is as follows:

$$E_{kin} = \frac{m v^2}{2e} \tag{5}$$

eV units are used for convenience. Using the previously estimated ion velocity we obtain:

$$E_{kin} = 3.25 \times 10^4\,\text{eV} \tag{6}$$

The collision energy in the center of mass (CM) reference frame:

$$E_{CM} = \frac{E_{kin} m_g}{(m + m_g)} = 106\,\text{eV} \tag{7}$$

Thus, the ion energy is sufficiently high that ion fragmentation can occur [21–23]. The CM energy is approximately independent of the ion molecular mass m, considering $m \gg m_g$ and $m/z \sim 1000$, characteristic for ESI multiply charged ions. For example, the 77+ charge state of bovine serum albumin ion (m = 66 kDa) will experience approximately same CM collision energy (106 eV) as the above ubiquitin 10+ ion, regardless of ~8 times difference in the molecular mass. The center of mass collision energy can be reduced using lighter neutral gas molecules. Replacing the nitrogen in the UHV chamber with helium (m_g = 4) results in CM energy of only 15 eV as calculated using previously defined parameters and equations. Similar experimental measurements to those reported here but with helium collision gas will be considered for future studies.

This high energy ion loss through fragmentation mechanism is similar to a high energy ejection mechanism, previously described theoretically by Arkin and Laude [19]. The mechanism proposed by Arkin and Laude was based on ion motion simulations using their own collision algorithm combined with SimIon (Scientific Instrument Services, Ringoes, NJ). While indeed such collision ejection mechanisms might have a significant role in the transient lifetime of relatively low molecular weight ions, for larger molecular weight ions, such as intact proteins, the ion fragmentation mechanism will have a more significant effect as fragmentation will occur prior to ion ejection.

3.3. Experimental confirmation of estimations

To examine the dependence of the signal lifetime on the time before a high energy collision, we have studied the excited coherent ion cloud signal lifetime at several different excitation powers. Fig. 5 shows the temporal dependence of the ion intensity corresponding to the maximum ubiquitin isotopic peak. This temporal dependence was calculated by Fourier-transforming the time domain data in eight 128k slices and normalizing the intensity to the transform of the first 128k data points. Higher charge states have proportionally increased ion velocities, Eq. (1)–(3), and thus have shorter times before an ion neutral collision, Eq. (3) (a more accurate treatment would include charge state specific cross sections [20]). This trend is clearly seen in Fig. 5 for all four excite power conditions shown, as increased excitation power corresponds to increased ion velocities, according to Eq. (1), and thus smaller t_{coll}.

As shown in Fig. 6, a characteristic signal lifetime, τ, can be calculated using an exponential fit to the signal decay curves in Fig. 5. Interestingly, the lifetime, τ of 0.5 s, for ubiquitin 10+ with an excitation attenuation of 3 dB is consistent with the above calculation, t_{coll} of 0.66 s (recall both the calculations and gas pressure readings are approximate). The near linear dependence of τ on $1/z$ with excitation attenuation of 3 dB is also consistent with the previous estimations. Note also in Fig. 6, the proportionally reduced signal lifetimes of ion signal at a UHV pressure of 3 compared to 1×10^{-10} Torr at the same excitation power (5 dB). The signal lifetime shows a super-linear behavior for lower charge states, z of 7 and 8, at low excitation powers, 7 and 9 dB (9 dB data not shown). This can be attributed to reduced kinetic energies corresponding to such conditions, $E_{CM} \lesssim 100$ eV, so that the contribution of the high energy fragmentation mechanism becomes relatively less significant compared to other mechanisms, and the transient lifetimes correspondingly increase.

To test this assumption, we have conducted a more detailed analysis on how the ion signal life time depends on the ion kinetic energy, i.e., in case of our measurements, the post-excitation radius. Fig. 7 shows excitation power (dB) profiles of the characteristic signal lifetime observed for ubiquitin charge states 8, 9 and 10+, for UHV pressure 3×10^{-10} Torr. A sharp transition is observed in the range 7–9 dB from short-lived signals at higher excitation powers (i.e., lower dB values) to long lifetimes at the optimal excitation powers. The more extended signals can be interpreted as a result of the ion kinetic energy decreasing below the threshold for an efficient single collision fragmentation. The ion-neutral collisions lead to a minor change in the ion velocity (in terms of both magnitude and direction) since the ratio of the ion molecular mass to the neutral mass is very high, in this case ~300. Thus, multiple ion-neutral collisions are needed to completely de-phase the ion ensemble, a result similar to simulations performed by Arkin and Laude [19]. Interestingly, the long-lasting signals were obtained at the excitation powers of low energy transition, regardless of the increased UHV pressure used for these measurements, 3×10^{-10} Torr. We specifically chose these experimental conditions since the observed range of signal lifetimes was consistent with the 1.3 s transients used. The normal UHV regime resulted in lifetimes far exceeding the transient length which made it difficult to clearly see the transition. The lifetime decline for dB values above optimal can be attributed to increased space charge effects with the smaller cyclotron radii. Overall, the behavior in Fig. 7 is consistent with the expected kinetic

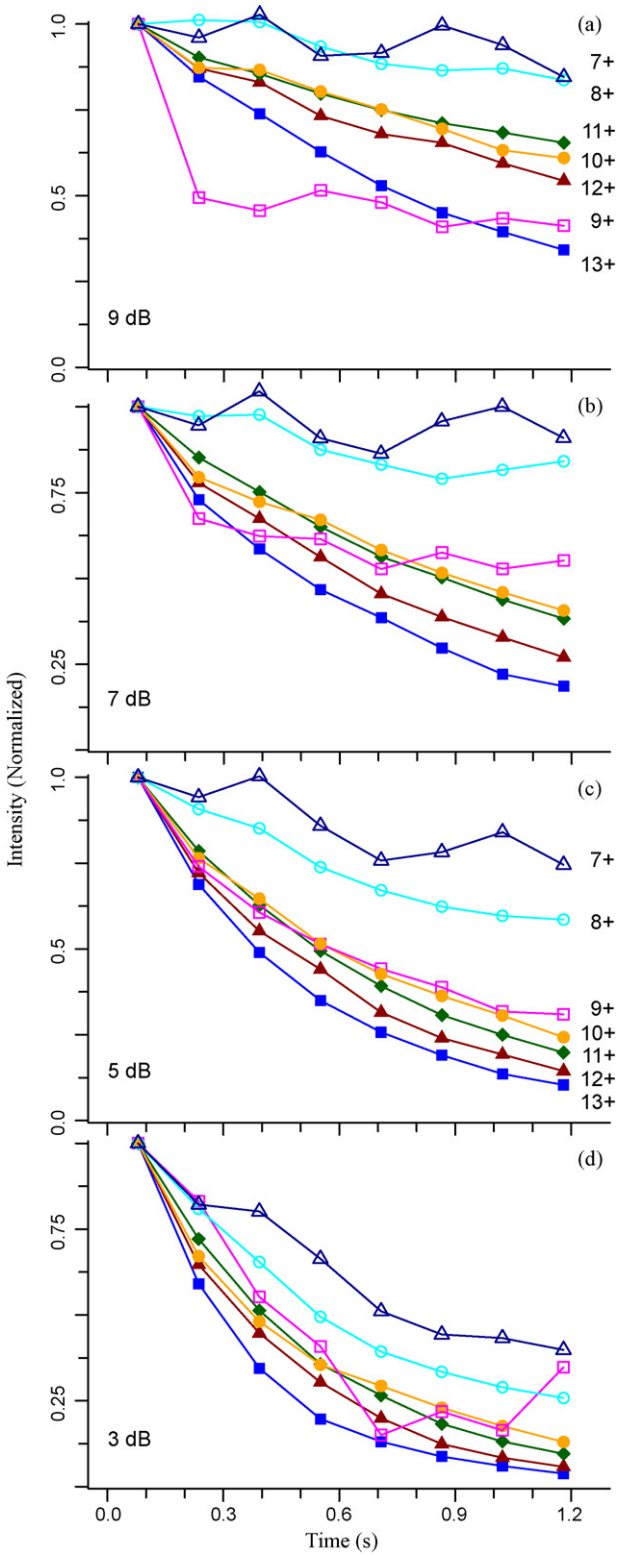

Fig. 5. Transient decay curves showing the intensity of the most abundant isotope peak for ubiquitin 7 to 13+ charge states versus time obtained by Fourier-transforming the full 1 M word transient in eight 128k word segments. Each transformed segment measures the ion signal obtained at a certain time point in the transient. The observed segment intensities were normalized to the intensity of the first segment for each charge state. Plots are shown for mass spectra obtained at excitation attenuations of (a) 9 dB, (b) 7 dB, (c) 5 dB and (d) 3 dB for ubiquitin 7+ (open triangles), 8+ (open circles), 9+ (open squares), 10+ (solid circles), 11+ (diamonds), 12+ (solid triangles), and 13+ (solid squares).

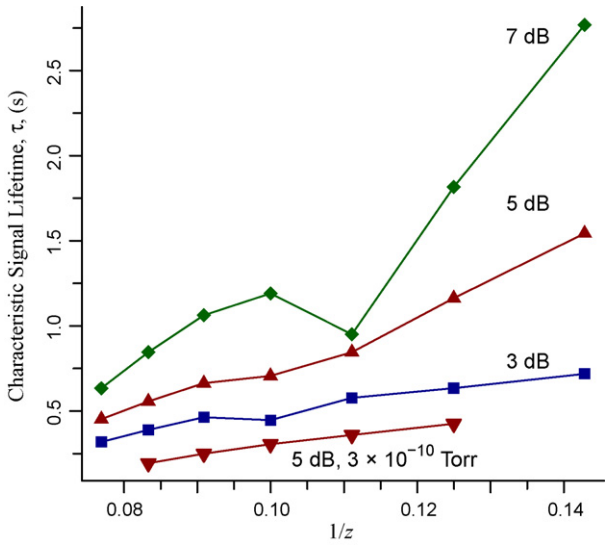

Fig. 6. The characteristic signal lifetime, τ, for ubiquitin charges states 7 to 13+ (plotted as $1/z$) calculated by fitting the transient decay curves (see Fig. 5) observed at 7 dB (diamonds), 5 dB (triangles), and 3 dB (squares) to an exponential function. Results from a pressure of ~1 (triangles pointing up) and 3 (triangles pointing down) $\times 10^{-10}$ Torr are shown for an excitation attenuation of 5 dB. Pressure for all others was $\sim 1 \times 10^{-10}$ Torr.

energy driven mechanism. The center of mass kinetic energy estimated for 10+ charge state at the transition, 9 dB, is $E_{CM} \approx 33$ eV. The curve for 8+ shows the transition at ~7 dB, corresponding to a very close CM energy of ≈33 eV, i.e., the kinetic energy reduction due to the lower charge state is compensated by an energy increase due to the greater excitation radius. This observation is consistent with the above assumption that the ion kinetic energy is the factor that determines the transition from short to long ion signal times.

3.4. Generalization of single collision ion fragmentation mechanism

The results obtained for ubiquitin ions can be generalized to larger molecular ions. Large ions require more collisions to pro-

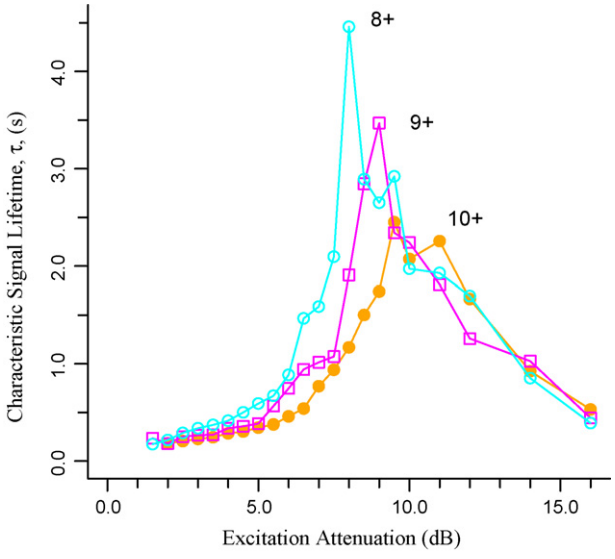

Fig. 7. The characteristic signal lifetime, τ, at different excitation power levels (in terms of attenuation dB) for ubiquitin 8+ (open circles), 9+ (squares), 10+ (solid circles), at a pressure 3×10^{-10} Torr.

duce a noticeable effect on the ion trajectory, whether due to ion-neutral scattering or due to ion dissociation produced by multiple ion-neutral collisions. The moderate post-excitation cyclotron radii generally required for high resolution FT-ICR measurements of large ions, $r_c \lesssim 1$ cm, ensure sufficiently low ion kinetic energies, so that sufficiently long signals can be obtained under conditions of multiple ion-neutral collisions. Thus, the successful FT-ICR observation of very large ions, e.g., >100 MDa [24], was possible under standard UHV conditions.

The situation is different when higher ion kinetic energies are used, so that the single collision ion dissociation can occur. It is not generally known how the single-collision dissociation energy threshold depends on the molecular mass for the large protein ions. For an approximate estimation one can assume that the center of mass threshold energies are similar to that obtained above for the ubiquitin ions, E_{CM} ~30 eV. Assuming the ion mass much larger than neutral mass, the center of mass collision energy is defined by the velocity of ion, Eq. (1). Under such assumptions, macromolecular ions of various sizes should experience the transition to the high energy, short lifetime regime at similar conditions, largely defined by the ion mass to charge ratio m/z and the post-excitation cyclotron radius r_c. Assuming the high kinetic energy regime with CM energy exceeding the single collision dissociation threshold, it can be expected that larger molecular ions having correspondingly increased cross sections will require proportionally lower vacuum in order to obtain long living signals.

Alternatively, if the high vacuum requirements cannot be achieved, mass spectra can be obtained with the low energy conditions. In this case, the dynamic range of measurements suffers from the reduced excitation radius, since the induced signal detected in FT-ICR is proportional to the ratio of the excite radius to the cell radius [25]. Even more critical, space charge effects increase inversely proportionally to the radius squared resulting in increased shear forces which act to de-phase low abundant ion components, such as ion populations corresponding to the small isotopic peaks at the edges of the isotope distribution. To offset the reduced dynamic range, accumulation of multiple spectra may be required under the low energy operation. Other methods to increase dynamic range such as pre-selection of a narrow m/z range [26] or selective ejection of high abundant ions [27] can also be effective.

Interestingly, the mechanism considered here can also be applied for Orbitrap mass analyzers which are based on an alternative FTMS technique [28]. The injection of ions into the Orbitrap defines the kinetic energy of ions during detection, fixed at ~2 keV per charge for 3.5 kV operation, independent of the ion mass to charge ratio [28]. This total kinetic energy of ions in the Orbitrap is close to the value estimated above for our FT-ICR measurements, when the high excitation power conditions are used, $r_c \approx 2$ cm: 3.2 kV per charge for 10+ ubiquitin ions, Eq. (6). In the Orbitrap, only the axial component of ion motion contributes to the detected signal, which corresponds to a fraction of the total ion kinetic energy, while close to 100% of the kinetic energy is used for detection in FT-ICR MS. The ion ensemble de-phasing due to collisions is defined by the total ion kinetic energy, so similar scales of the pressure-determined signal lifetime can be expected for Orbitrap. (We intentionally simplify the comparison, since the full treatment including a consideration of different space and image charge configurations, cohesive forces due to the magnetic field, and other specifics of the two FTMS techniques, falls far beyond the scope of this study). It should be noted that a relatively small range of z oscillations in Orbitrap, ±5 mm, is sufficient for detection of the induced signal, due to the compact dimensions of the Orbitrap cell. (Note that the robustness of the Orbitrap to space charge effects [29] permits using the relatively compact Orbitrap cell dimensions).

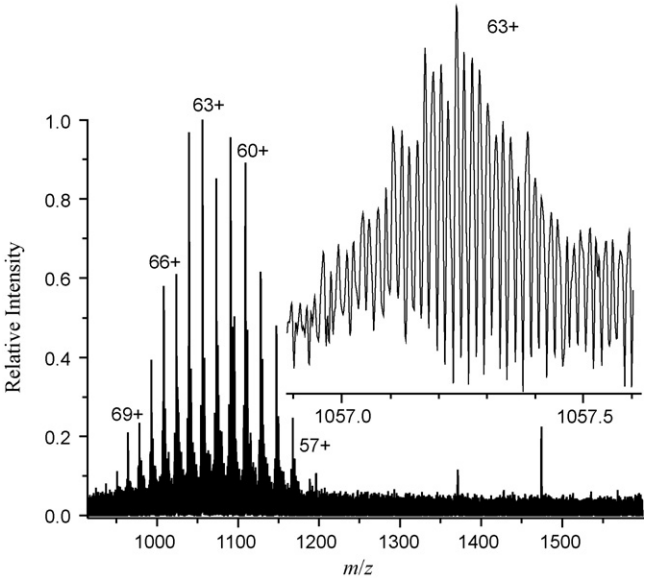

Fig. 8. LC-MS mass spectra of bovine serum albumin (BSA) obtained by summing 50 scans of the BSA LC peak. Several isoforms with various adducts were observed and the base peak of the 63+ cluster is shown in the insert.

A newly developed high field Orbitrap utilizes an electric field up to 2 times higher than previous Orbitrap mass analyzers due to decreased gap distance between electrodes with a high voltage increased to 5 kV [29]. Isotopically resolved spectra of proteins up to ~50 kDa can be obtained using accumulation of multiple spectra, thanks to improved pressure conditions, $<1 \times 10^{-10}$ Torr. A key requirement for Orbitrap performance is the precise manufacturing of the Orbitrap cell electrodes [29], the closed geometry of which should create a challenge for a radical reduction of the UHV pressure. The current pressures within the Orbitrap cell result from a remarkable engineering feat to achieve UHV range pressures considering that the high pressure (~1 mTorr) C-trap is positioned just centimeters away.

Considering the relatively high ion kinetic energies used in the Orbitrap mass analyzers, we expect that a further optimization of the technique for high molecular weight ions should face a similar choice of either creating nearly collision-free conditions during detection or reducing the ion kinetic energy below the threshold of the single-collision ion fragmentation. It should be noted that with the "excitation by injection" method currently employed in Orbitrap mass analyzers, the total ion kinetic energy during detection is fully determined by the high voltage applied to the central electrode, since the geometry of the ion cloud has fixed axial and radial dimensions. Thus, adjusting to lower ion energies can only be done by reducing the high voltage. A recent report for ~50 kDa protein mass spectra used the high voltage reduced by factor of 2, from 5 to 2.5 kV [29]. Reducing the voltage results in the reduction of the detected ion frequencies proportionally to the square root of the voltage [30], effectively diminishing the mass resolution. This is different from FT-ICR, where the ion kinetic energy can be adjusted using reduced excitation radii, with just a negligible effect on the characteristic ion frequencies.

To aid in illustrating the application of these estimations to ever larger target proteins consider the case of LC-MS mass spectra for BSA, as shown in Fig. 8. BSA has an m of 66 kDa and z of 57–70, thus a shorter average time before an ion neutral collision after excitation. The cross section of BSA ions is ~10 times larger than the cross section of ubiquitin [31], making it problematic to create vacuum conditions for the high excitation power mode to be

effective. This increased cross section of larger proteins, such as BSA, is partially offset by fragmenting at increased collision energies. Increasing the size of molecules also increases the number of internal degrees of freedom which essentially allows energy, such as from an ion neutral collision, to be dissipated into many more channels effectively increasing the energy required for dissociation [21–23]. Apparently, the increased dissociation energy is insufficient to compensate for the increased collision cross section and increased excitation energy (due to increased charge states) and currently, the optimal mass spectra for BSA were obtained in the low energy regime, using reduced excitation powers (9 dB).

This demonstrates the complex interplay between sensitivity, MMA, and resolution in the analysis of larger macro-molecules, such as BSA [13,32]. Obviously, in the analysis of such systems, the improved sensitivity and MMA at higher excitation powers is desirable. However, the decreased resolution at higher excitation powers can make resolving the isotope distribution challenging. While the resolution of ~100,000 in Fig. 8 is sufficient for determining the charge state from the isotope distribution, larger proteins will require increased resolution to observe resolved isotopic structures. We are continuing to investigate the performance and optimization of the compensated cell for large molecular systems and further UHV improvement should have a significant impact for obtaining better quality results for the larger proteins.

4. Conclusion

We report optimization of the 12 T FT-ICR mass spectrometer for the analysis of large macro-molecular ions, such as proteins. The instrument was upgraded with a compensated open cylindrical ion trapping cell that enabled improved sensitivity, dynamic range, and mass measurement accuracy, due to the modified trapping potential of the cell which closely approximates the ideal harmonic trapping potential. Single transient spectra of multiply charged bovine ubiquitin ions showed sub-ppm mass measurement accuracy, along with improved signal intensity and dynamic range, under conditions of increased post-excitation cyclotron radii available with the new cell. An outcome of the increased cyclotron radii is increased ion kinetic energy, which can result in ion fragmentation from a single ion neutral collision. A transition can occur from relatively long signal lifetimes at low excitation radii to shorter lifetimes, defined by the average ion-neutral collision time, for excitation powers high enough for the single collision ion loss. Data presented herein are consistent with the proposed signal lifetime treatment that suggests a critical role of the total ion kinetic energy for obtaining optimal conditions for the high resolution measurements of large molecular ions. The observation is consistent with previous studies indicating that high ion kinetic energy makes the vacuum requirement more severe [29,33]. Continued improvement of the FTMS technology involves using higher characteristic frequencies of ion motion, which permits higher mass resolution achievable with shorter signal acquisition times. With FT-ICR this can be achieved using higher magnetic fields, while with Orbitrap, a further increase of the electric field is used. In both cases, the kinetic energy of ions increases substantially and can reach a threshold where just a single ion-neutral collision is sufficient to exclude an ion from the coherent ion ensemble. Similar ion kinetic energy scales are used for conditions generally employed for FT-ICR and Orbitrap mass analyzers. While the high kinetic energy operation was optimal for compounds of a moderate size, less than ~10 kDa, for higher molecular weight compounds such as BSA, using increased excitation radii resulted in reduced transient lifetimes, thus reduced excitation powers were used, consistent with the considered mechanism. Under the reduced excitation power operation reduced sensitivity and dynamic range and increased space charge related mass measurement errors were observed, and accumulation of multiple transients was necessary. Thus, further reductions in UHV pressure are expected to enable the benefits of increased excitation power to be applied to the analysis of larger macro-molecular ions of interest.

Acknowledgements

The authors gratefully acknowledge Dr. J. Laskin for helpful discussions. Portions of this work were supported by the National Center for Research Resources (RR 018522), the National Institute of Allergy and Infectious Diseases (NIH/DHHS through interagency agreement Y1-AI-4894-01), the National Institute of General Medical Sciences (NIGMS, R01 GM063883), and the U. S. Department of Energy (DOE) Office of Biological and Environmental Research. Work was performed in the Environmental Molecular Science Laboratory, a DOE national scientific user facility located on the campus of Pacific Northwest National Laboratory (PNNL) in Richland, Washington. PNNL is a multi-program national laboratory operated by Battelle for the DOE under Contract DE-AC05-76RLO 1830.

References

[1] S.H. Guan, A.G. Marshall, S.E. Scheppele, Anal. Chem. 68 (1996) 46.
[2] Z.G. Wu, R.P. Rodgers, A.G. Marshall, Fuel 84 (2005) 1790.
[3] Z.G. Wu, R.P. Rodgers, A.G. Marshall, J. Agric. Food Chem. 52 (2004) 5322.
[4] Z. Takats, V. Kobliha, K. Sevcik, P. Novak, G. Kruppa, K. Lemr, V. Havlicek, J. Mass Spectrom. 43 (2008) 196.
[5] S.C. Brown, G. Kruppa, J.L. Dasseux, Mass Spectrom. Rev. 24 (2005) 223.
[6] R.D. Smith, Int. J. Mass Spectrom. 200 (2000) 509.
[7] M. Bohac, A. Ingendoh, J. Fuchser, M. Witt, Chem. Listy 99 (2005) 943.
[8] S.A. Hofstadler, J.C. Severs, R.D. Smith, F.D. Swanek, A.G. Ewing, Rapid Commun. Mass Spectrom. 10 (1996) 919.
[9] N.L. Kelleher, Anal. Chem. 76 (2004) 196A.
[10] J.L. Benesch, C.V. Robinson, Curr. Opin. Struct. Biol. 16 (2006) 245.
[11] S. Sharma, D.C. Simpson, N. Tolić, N. Jaitly, A.M. Mayampurath, R.D. Smith, L. Paša-Tolić, J. Proteome Res. 6 (2007) 602.
[12] H.S. Smallwood, N.M. Lourette, C.B. Boschek, D.J. Bigelow, R.D. Smith, L. Paša-Tolić, T.C. Squier, Biochemistry 46 (2007) 10498.
[13] N.L. Kelleher, M.W. Senko, M.M. Siegel, F.W. McLafferty, J. Am. Soc. Mass Spectrom. 8 (1997) 380.
[14] A.V. Tolmachev, E.W. Robinson, S. Wu, H. Kang, N.M. Lourette, L. Paša-Tolić, R.D. Smith, J. Am. Soc. Mass Spectrom. 19 (2008) 586.
[15] V.H. Vartanian, F. Hadjarab, D.A. Laude, Int. J. Mass Spectrom. 151 (1995) 175.
[16] S.C. Beu, D.A. Laude, Anal. Chem. 64 (1992) 177.
[17] G. Gabrielse, L. Haarsma, S.L. Rolston, Int. J. Mass Spectrom. Ion Process. 88 (1989) 319.
[18] S.H. Guan, A.G. Marshall, Int. J. Mass Spectrom. Ion Process. 146 (1995) 261.
[19] C.R. Arkin, D.A. Laude, J. Am. Soc. Mass Spectrom. 16 (2005) 422.
[20] J.W. Li, J.A. Taraszka, A.E. Counterman, D.E. Clemmer, Int. J. Mass Spectrom. 187 (1999) 37.
[21] J. Laskin, in: J. Laskin, C. Lifshitz (Eds.), Principles of Mass Spectrometry Applied to Biomolecules, John Wiley & Sons, Inc, 2006, p. 619.
[22] V.J. Nesatyy, J. Laskin, Int. J. Mass Spectrom. 221 (2002) 245.
[23] J. Laskin, J.H. Futrell, Mass Spectrom. Rev. 22 (2003) 158.
[24] R.D. Chen, X.H. Cheng, D.W. Mitchell, S.A. Hofstadler, Q.Y. Wu, A.L. Rockwood, M.G. Sherman, R.D. Smith, Anal. Chem. 67 (1995) 1159.
[25] A.G. Marshall, C.L. Hendrickson, G.S. Jackson, Mass Spectrom. Rev. 17 (1998) 1.
[26] R.L. Wong, I.J. Amster, J. Am. Soc. Mass Spectrom. 17 (2006) 205.
[27] R. Harkewicz, M.E. Belov, G.A. Anderson, L. Paša-Tolić, C.D. Masselon, D.C. Prior, H.R. Udseth, R.D. Smith, J. Am. Soc. Mass Spectrom. 13 (2002) 144.
[28] Q.Z. Hu, R.J. Noll, H.Y. Li, A. Makarov, M. Hardman, R.G. Cooks, J. Mass Spectrom. 40 (2005) 430.
[29] A. Makarov, E. Denisov, O. Lange, W. Balschun, J. Griep-Raming, 56th ASMS Conference on Mass Spectrometry & Allied Topics, Denver, Colorado, 2008.
[30] A. Makarov, Anal. Chem. 72 (2000) 1156.
[31] T. Covey, D.J. Douglas, J. Am. Soc. Mass Spectrom. 4 (1993) 616.
[32] M.V. Gorshkov, L. Paša-Tolić, G.A. Anderson, B.M. Huang, J.E. Bruce, D.C. Prior, S.A. Hofstadler, L.A. Tang, L.Z. Chen, J.A. Willett, A.L. Rockwood, M.S. Sherman, R.D. Smith, J. Am. Soc. Mass Spectrom. 9 (1998) 692.
[33] T.M. Schaub, C.L. Hendrickson, S. Horning, J.P. Quinn, M.W. Senko, A.G. Marshall, Anal. Chem. 80 (2008) 3985.